Two-Dimensional Precoding for 3D Massive MIMO

Zhaocheng Wang, *Senior Member, IEEE*, Wendong Liu, Chen Qian, Sheng Chen, *Fellow, IEEE*, and Lajos Hanzo, *Fellow, IEEE*

***Abstract*—A two-dimensional (2D) precoding scheme is proposed for three-dimensional massive multiple-input multiple-output (3D MIMO) systems to efficiently exploit the 2D antenna array of the base station. Specifically, by exploiting the Kronecker structure of the 3D MIMO channel matrix, the transmit precoding operation is divided into elevation precoding and azimuth precoding. Explicitly, in contrast to the existing beamforming schemes, precoding is also performed in the vertical dimension. Consequently, the proposed scheme can fully exploit the extra degrees of freedom provided by the vertical dimension for avoiding the inter-user interference so as to improve the attainable system performance. Compared to the conventional scheme relying on the equivalent one-dimensional precoding, the proposed 2D precoding scheme offers an improved performance in severe inter-cell interference-contaminated environments, despite its lower complexity.**

***Index Terms*—3D massive MIMO, Kronecker structure, inter-user interference, precoding, 2D precoding**

I. Introduction

Massive multiple-input multiple-output (MMIMO) arrangements have attracted considerable attention as a benefit of their potential of significantly increasing the spectral efficiency and/or the energy efficiency by relying on low-complexity linear signal processing schemes [1]–[4]. However, most studies focus on the classic uniformly-spaced linear array (ULA), which is not suitable for practical MMIMO systems relying on a large antenna array. Three-dimensional massive MIMOs (3D MMIMO) [5], [6], also often referred to as full-dimensional MIMOs are capable of overcoming this dimensionality problem of the base station (BS), since the array size can be reduced when the elevation domain represented by the vertical dimension is also exploited. This way 3D MMIMOs create extra degrees of freedom for avoiding the inter-cell interference, while achieving an improved spectral efficiency. However, given the same total number of antenna elements at the BS, two-dimensional (2D) uniformly-spaced rectangular arrays (URA) perform worse than the ULA due to their low resolution in the elevation domain [5], and thus either vertical beamforming or transmit precoding (TPC) has to be invoked for improving the performance of 3D MIMO systems [7]–[9].

Z. Wang, W. Liu and C. Qian are with Tsinghua National Laboratory for Information Science and Technology, Department of Electronic Engineering, Tsinghua University, Beijing 100084, China (E-mails: zcwang@tsinghua.edu.cn; lwd15@mails.tsinghua.edu.cn; qianc10@mails.tsinghua.edu.cn).

S. Chen and L. Hanzo are with Electronics and Computer Science, University of Southampton, Southampton SO17 1BJ, U.K. (E-mails: sqc@ecs.soton.ac.uk, lh@ecs.soton.ac.uk). S. Chen is also with King Abdulaziz University, Jeddah 21589, Saudi Arabia.

This work was supported by National Key Basic Research Program of China (No.2013CB329203), National Nature Science Foundation of China (No.61571267), Beijing Natural Science Foundation (No.4142027), National High Technology Research and Development Program of China (No.2014AA01A704), Shenzhen Visible Light Communication System Key Laboratory (ZDSYS20140512114229398) and Shenzhen Peacock Plan (No.1108170036003286).

A pair of existing approaches, which beneficially exploit the extra degrees of freedom introduced by the 2D antenna array are constituted by beamforming and multiplexing. The first approach relies on performing beamforming in the elevation domain and then invokes TPC in the equivalent azimuth domain [7], [8]. The Kronecker structure of the 3D MIMO channel matrix is exploited and based on the approximated elevation-domain steering vector, eigen-beamforming is invoked by relying on the eigenvector corresponding to the largest eigenvalue of the elevation-domain channel's correlation matrix as the beamforming vector. As the number of antennas in the elevation domain tends to infinity, the beam becomes sufficiently narrow for the inter-user interference to be mitigated [9], [10], but it still cannot be completely eliminated, which degrades the overall performance.

The second approach adopts the conventional TPC algorithm [2], [3] based on the vectorial form of the 3D MMIMO channel matrix, where the structure of 3D MIMO channel is not exploited. This full TPC approach suffers from the drawback of a potentially excessive complexity imposed by the TPC matrix computation. Furthermore, this full TPC algorithm is only optimal for an unrealistic single-cell senario, i.e. in the absence of inter-cell interference. By contrast, in hostile inter-cell interference-infested environments its performance may actually be worse than that the beamforming scheme, as it will be shown in our simulation study.

Against this backcloth, in this correspondence, we propose a 2D TPC scheme for 3D MMIMOs for eliminating the inter-user interference. In contrast to both the conventional beamforming scheme of [7], as well as to the multi-layer precoding algorithm of [8] and to the existing full TPC scheme of [2], [3], our arrangement performs precoding in both the elevation and azimuth domains based on the Kronecker structure of the 3D MIMO channel matrix. Specifically, the extra degrees of freedom introduced by the elevation-oriented antennas is fully exploited for distinguishing the different users roaming in the cell illuminated. As a result, the inter-user interference can be completely eliminated by a finite number of elevation-domain antennas. Hence the overall system performance is significantly improved in comparison to the conventional beamforming scheme. Compared to the conventional full precoding scheme, the proposed 2D precoding scheme is capable of significantly outperforming the former in hostile inter-cell interference-contaminated environments, despite its complexity. We emphasize that in the literature, the Kronecker structure of the 3D MIMO channel matrix has been exploited for conceiving efficient channel state information feedback schemes [11]–[13]. However, to the best of our knowledge, we are the first to propose this 2D TPC scheme, which efficiently exploits the Kronecker structure of the 3D MMIMO channel matrix to perform TPC both in the elevation- and azimuth-

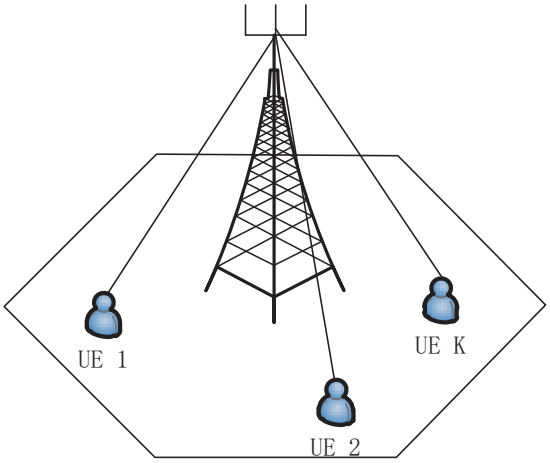

Fig. 1. Illustration of single-cell multi-user scenario.

domains.

This correspondence is organized as follows. Section II discusses the downlink system model and the Kronecker structure of the 3D MIMO channel matrix. Section III presents the proposed 2D TPC scheme conceived for 3D MMIMOs, including the detailed mathematical analysis of its efficiency. Our simulation results are provided in Section IV for demonstrating the superior performance of this 2D precoding scheme over the existing beamforming and full TPC approaches. Our concluding remarks are drawn in Section V.

II. System Model and Kronecker Structure

For simplicity of illustration, let us consider the single-cell scenario supporting K single-antenna aided users as seen in Fig. 1, noting that our scheme is equally applicable to multi-cell scenarios. The BS employs a URA having M_y and M_x antennas in the elevation- and azimuth-domains, respectively. The number of antennas at the BS is thus $M = M_y M_x$. Let D_y and D_x be the antenna spacings in the elevation and azimuth domains, respectively. We assume that $D_x = D_y = D$. Let us furthermore denote the downlink channel matrix between the BS and the k-th user by $\mathbf{H}_k = \left[\mathbf{h}_{k,1}\ \mathbf{h}_{k,2}\cdots\mathbf{h}_{k,M_y}\right]^{\mathrm{T}} \in \mathbb{C}^{M_y\times M_x}$, where $\mathbf{h}_{k,l}^{\mathrm{T}} \in \mathbb{C}^{1\times M_x}$ is the l-th row of $\mathbf{H}_k$ and $(\ )^{\mathrm{T}}$ denotes the transpose operator. An equivalent vectorial form of $\mathbf{H}_k$ is $\mathbf{h}_{\mathrm{vec},k} = \left[\mathbf{h}_{k,1}^{\mathrm{T}}\ \mathbf{h}_{k,2}^{\mathrm{T}}\cdots\mathbf{h}_{k,M_y}^{\mathrm{T}}\right]^{\mathrm{T}} \in \mathbb{C}^{(M_xM_y)\times 1}$. Denote $\mathbf{x} = \left[x_1\ x_2\cdots x_K\right]^{\mathrm{T}}$ with $E\{\mathbf{x}\mathbf{x}^{\mathrm{H}}\} = \mathbf{I}_K$, which contains the symbols transmitted by the BS to the K users, where $(\ )^{\mathrm{H}}$ is the conjugate transpose operator and $E\{\ \}$ denotes the expectation. The received signal vector $\mathbf{r} = \left[r_1\ r_2\cdots r_K\right]^{\mathrm{T}} \in \mathbb{C}^{K\times 1}$ by the K users can be expressed as

$$\mathbf{r} = \mathbf{H}_{\mathrm{vec}}\mathbf{W}_{\mathrm{vec}}\mathbf{x} + \mathbf{n}, \tag{1}$$

where $\mathbf{n} = \left[n_1\ n_2\cdots n_K\right]^{\mathrm{T}} \in \mathbb{C}^{K\times 1}$ is the additive white Gaussian noise (AWGN) vector experienced in the downlink and $\mathbf{H}_{\mathrm{vec}} = \left[\mathbf{h}_{\mathrm{vec},1}\ \mathbf{h}_{\mathrm{vec},2}\cdots\mathbf{h}_{\mathrm{vec},K}\right]^{\mathrm{T}} \in \mathbb{C}^{K\times(M_xM_y)}$ is the downlink channel matrix between the BS and the K users, while $\mathbf{W}_{\mathrm{vec}} = \left[\mathbf{w}_{\mathrm{vec},1}\ \mathbf{w}_{\mathrm{vec},2}\cdots\mathbf{w}_{\mathrm{vec},K}\right] \in \mathbb{C}^{(M_xM_y)\times K}$ is the precoding matrix associated with $\mathbf{w}_{\mathrm{vec},k} \in \mathbb{C}^{(M_xM_y)\times 1}$ being the TPC vector for the k-th user. Hence, the received signal of the k-th user is given by

$$r_k = \mathbf{h}_{\mathrm{vec},k}^{\mathrm{T}}\mathbf{w}_{\mathrm{vec},k}x_k + \sum_{k'\neq k}\mathbf{h}_{\mathrm{vec},k}^{\mathrm{T}}\mathbf{w}_{\mathrm{vec},k'}x_{k'} + n_k. \tag{2}$$

The second term in the right hand side of (2) represents the inter-user interference, also known as intra-cell interference, and $\mathbf{W}_{\mathrm{vec}}$ is designed to eliminate this interference or to make it negligibly small. Note that in a multi-cell environment, there will also be an inter-cell interference component in r_k and it becomes vital to ensure that the matrix $\mathbf{W}_{\mathrm{vec}}$ reduces this inter-cell interference.

We consider the following narrow-band multi-path channel model [14]

$$\mathbf{H}_k = \sum_{p=1}^{P}\mathbf{H}_k^p, \tag{3}$$

where P is the number of paths and $\mathbf{H}_k^p \in \mathbb{C}^{M_y\times M_x}$ is the channel matrix of the p-th path. The element at the l-th row and m-th column of $\mathbf{H}_k^p$ is given by [11]

$$\begin{aligned} h_k^{m,l,p} =& \rho_k^p e^{-\mathrm{j}2\pi\frac{D}{\lambda}\left((m-1)\cos\theta_k^p\cos\beta_k^p + (l-1)\sin\beta_k^p\right)} \\ =& \rho_k^p e^{-\mathrm{j}2\pi\frac{(m-1)D}{\lambda}\cos\theta_k^p\cos\beta_k^p} e^{-\mathrm{j}2\pi\frac{(l-1)D}{\lambda}\sin\beta_k^p} \\ =& \rho_k^p h_{\mathrm{a},k}^{m,p} h_{\mathrm{e},k}^{l,p}, \end{aligned} \tag{4}$$

where λ denotes the wavelength, θ_k^p is the angle-of-arrival in the azimuth domain (A-AOA), β_k^p is the angle-of-arrival in the elevation domain (E-AOA) and ρ_k^p is the large-scale fading coefficient of the p-th path, while $h_{\mathrm{a},k}^{m,p} = e^{-\mathrm{j}2\pi\frac{(m-1)D}{\lambda}\cos\theta_k^p\cos\beta_k^p}$ and $h_{\mathrm{e},k}^{l,p} = e^{-\mathrm{j}2\pi\frac{(l-1)D}{\lambda}\sin\beta_k^p}$ denote the azimuth and elevation components of $h_k^{m,l,p}$, respectively. Observe from (4) that $\mathbf{H}_k^p$ has the following Kronecker structure

$$\mathbf{H}_k^p = \rho_k^p\left(\mathbf{h}_{\mathrm{a},k}^p\right)^{\mathrm{T}} \otimes \mathbf{h}_{\mathrm{e},k}^p, \tag{5}$$

in which $\otimes$ denotes the Kronecker product operator,

$$\mathbf{h}_{\mathrm{a},k}^p = \left[1\ h_{\mathrm{a},k}^{1,p}\cdots h_{\mathrm{a},k}^{m,p}\cdots h_{\mathrm{a},k}^{(M_x-1),p}\right]^{\mathrm{T}} \tag{6}$$

and

$$\mathbf{h}_{\mathrm{e},k}^p = \left[1\ h_{\mathrm{e},k}^{1,p}\cdots h_{\mathrm{e},k}^{l,p}\cdots h_{\mathrm{e},k}^{(M_y-1),p}\right]^{\mathrm{T}} \tag{7}$$

are the azimuth- and elevation-domain steering vectors, respectively. The overall channel matrix can then be written as

$$\mathbf{H}_k = \sum_{p=1}^{P}\rho_k^p\left(\mathbf{h}_{\mathrm{a},k}^p\right)^{\mathrm{T}} \otimes \mathbf{h}_{\mathrm{e},k}^p. \tag{8}$$

Under the assumption that the angular spread of E-AOA is small, which is reasonable since compared to the height of the BS, the distance between the BS and the user is high, we have $\mathbf{h}_{\mathrm{e},k}^p \approx \mathbf{h}_{\mathrm{e},k}$ for $1 \le p \le P$, with $\mathbf{h}_{\mathrm{e},k}$ as the approximated elevation-domain steering vector. Thus $\mathbf{H}_k$ can be approximated by

$$\mathbf{H}_k \approx \left(\sum_{p=1}^{P}\rho_k^p\left(\mathbf{h}_{\mathrm{a},k}^p\right)^{\mathrm{T}}\right) \otimes \mathbf{h}_{\mathrm{e},k}. \tag{9}$$

The existing beamforming scheme [7] is based on the approximated elevation steering vector $\mathbf{h}_{\mathrm{e},k}$. This scheme first performs eigen-beamforming in the elevation-domain and then performs TPC in the azimuth-domain by exploiting the equivalent azimuth-domain steering vector obtained by eigen-beamforming. Let $\mathbf{R}_{\mathrm{e}} = E\{\mathbf{h}_{\mathrm{e},k}\mathbf{h}_{\mathrm{e},k}^{\mathrm{H}}\}$ be the correlation matrix in the elevation-domain, which is subjected to eigen-decomposition. The eigenvector corresponding to the largest eigenvalue of $\mathbf{R}_{\mathrm{e}}$ is chosen as the beamforming vector. In fact, this approximation may not completely conform to some communication scenarios according to 3D channel measurements results, which leads to some performance loss [15].

On the other hand, the conventional full TPC scheme [2], [3] directly calculates the precoding matrix based on the channel matrix $\mathbf{H}_k$ or its vectorial form of $\mathbf{h}_{\mathrm{vec},k}$ and does not exploit the Kronecker structure of the channel matrix (8). As a result, the computational complexity of this conventional full TPC scheme is high, on the order of M_xM_y, which is denoted as $\mathsf{O}\big(M_xM_y\big)$. This full TPC scheme is known to be efficient in terms of combating the inter-user interference and it is optimal in the single-cell environment. However, in a multi-cell senario subjected to strong inter-cell interference, the achievable performance of this full TPC scheme may actually be worse than that of the conventional beamforming scheme, as it will be shown later in our simulation study.

III. Two-Dimensional Precoding Scheme

This section details our proposed 2D precoding scheme conceived for 3D MMIMOs, which is capable of eliminating the inter-user interference, while maintaining a significantly lower computational complexity than the existing full precoding scheme.

A. Proposed Scheme

The idea is to perform elevation- and azimuth-domain TPC separately by exploiting the Kronecker structure of the approximate channel matrix (9). First, the approximated elevation-domain channel vector $\overline{\mathbf{h}}_{\mathrm{e},k}$ is obtained from the estimation of the coefficients between the k-th user and any column of the 2D antenna array. Then we calculate the elevation-domain precoding vector based on $\overline{\mathbf{h}}_{\mathrm{e},k}$. For the generic multi-user scenario, the elevation-domain channel matrix is constructed as

$$\overline{\mathbf{H}}_{\mathrm{e}} = \big[\overline{\mathbf{h}}_{\mathrm{e},1}\ \overline{\mathbf{h}}_{\mathrm{e},2}\cdots\overline{\mathbf{h}}_{\mathrm{e},K}\big]^{\mathrm{T}} \in \mathbb{C}^{K\times M_y}. \tag{10}$$

When the zero-forcing (ZF) precoding algorithm is used, the elevation-domain TPC matrix is calculated as

$$\mathbf{W}_{\mathrm{e}} = \overline{\mathbf{H}}_{\mathrm{e}}^{\mathrm{H}}\big(\overline{\mathbf{H}}_{\mathrm{e}}\overline{\mathbf{H}}_{\mathrm{e}}^{\mathrm{H}}\big)^{-1}\mathbf{\Gamma}_{\mathrm{e}} \in \mathbb{C}^{M_y\times K}, \tag{11}$$

where $\mathbf{\Gamma}_{\mathrm{e}} = \mathrm{diag}\{\gamma_{\mathrm{e},1},\gamma_{\mathrm{e},2},\cdots,\gamma_{\mathrm{e},K}\} \in \mathbb{C}^{K\times K}$ is a diagonal matrix for the normalization of the precoding matrix, and $\mathbf{W}_{\mathrm{e}} = \big[\mathbf{w}_{\mathrm{e},1}\ \mathbf{w}_{\mathrm{e},2}\cdots\mathbf{w}_{\mathrm{e},K}\big]$ with $\mathbf{w}_{\mathrm{e},k} \in \mathbb{C}^{M_y\times 1}$ being the TPC vector of the k-th user.

Then the equivalent azimuth-domain channel vector is obtained based on $\mathbf{H}_k$ and $\mathbf{w}_{\mathrm{e},k}$. Specifically, the equivalent azimuth-domain channel vector $\mathbf{h}_{\mathrm{a},k}^{eq} \in \mathbb{C}^{M_x\times 1}$ of the k-th user is given by

$$\mathbf{h}_{\mathrm{a},k}^{eq} = \mathbf{H}_k^{\mathrm{T}}\mathbf{w}_{\mathrm{e},k}. \tag{12}$$

Next the azimuth-domain TPC vector is calculated based on $\mathbf{h}_{\mathrm{a},k}^{eq}$. Applying the ZF TPC algorithm to the equivalent azimuth-domain channel matrix

$$\mathbf{H}_{\mathrm{a}}^{eq} = \big[\mathbf{h}_{\mathrm{a},1}^{eq}\ \mathbf{h}_{\mathrm{a},2}^{eq}\cdots\mathbf{h}_{\mathrm{a},K}^{eq}\big]^{\mathrm{T}} \in \mathbb{C}^{K\times M_x} \tag{13}$$

yields the azimuth-domain TPC matrix

$$\mathbf{W}_{\mathrm{a}} = \big(\mathbf{H}_{\mathrm{a}}^{eq}\big)^{\mathrm{H}}\Big(\mathbf{H}_{\mathrm{a}}^{eq}\big(\mathbf{H}_{\mathrm{a}}^{eq}\big)^{\mathrm{H}}\Big)^{-1}\mathbf{\Gamma}_{\mathrm{a}} \in \mathbb{C}^{M_x\times K}, \tag{14}$$

where $\mathbf{\Gamma}_{\mathrm{a}} = \mathrm{diag}\{\gamma_{\mathrm{a},1},\gamma_{\mathrm{a},2},\cdots,\gamma_{\mathrm{a},K}\} \in \mathbb{C}^{K\times K}$ is a diagonal matrix for the normalization of the precoding matrix, and $\mathbf{W}_{\mathrm{a}} = \big[\mathbf{w}_{\mathrm{a},1}\ \mathbf{w}_{\mathrm{a},2}\cdots\mathbf{w}_{\mathrm{a},K}\big]$ with $\mathbf{w}_{\mathrm{a},k} \in \mathbb{C}^{M_x\times 1}$ being the azimuth precoding vector for the k-th user.

Finally, the overall TPC matrix of the k-th user is constructed as

$$\mathbf{W}_k = \mathbf{w}_{\mathrm{a},k}^{\mathrm{T}} \otimes \mathbf{w}_{\mathrm{e},k} \in \mathbb{C}^{M_y\times M_x}. \tag{15}$$

Table I summarizes the procedure of this 2D TPC scheme. Based on the TPC matrix $\mathbf{W}_k$ of (15), the received signal r_k of the k-th user will not be contaminated by the other users in the same cell, and our 2D TPC algorithm has a low complexity. We justify the efficiency of our proposal and its low complexity in the next two subsections.

B. Performance Analysis

We prove that based on the TPC matrix $\mathbf{W}_k$ (15), the inter-user interference imposed on the received signal r_k can be eliminated in the single-cell scenario, when encountering the ideal MIMO channel (9), i.e., $\mathbf{h}_{\mathrm{e},k}^{p} = \mathbf{h}_{\mathrm{e},k}$ for $1 \le p \le P$. Let $H_k^{(l,m)}$ and $W_k^{(l,m)}$ be the l-th row and m-th column elements of $\mathbf{H}_k$ and $\mathbf{W}_k$, respectively. Furthermore, let us define the operator $\oplus$ as the 'inner product' of two matrices according to

$$\mathbf{H}_k \oplus \mathbf{W}_k = \sum_{m=0}^{M_x-1}\sum_{l=0}^{M_y-1} H_k^{(l,m)}W_k^{(l,m)}. \tag{16}$$

Let $w_{\mathrm{a},k}^{m}$ be the m-th term of the azimuth TPC vector $\mathbf{w}_{\mathrm{a},k}$. Bearing in mind $\mathbf{H}_k$ of (9) and $\mathbf{W}_k$ of (15), we have

$$\begin{aligned}\mathbf{H}_k \oplus \mathbf{W}_k =& \sum_{m=0}^{M_x-1}\Big(\sum_{p=1}^{P}\big(\rho_k^p h_{\mathrm{a},k}^{m,p}\mathbf{h}_{\mathrm{e},k}^{\mathrm{T}}\big)\big(w_{\mathrm{a},k}^{m}\mathbf{w}_{\mathrm{e},k}\big)\Big)\\ =&\mathbf{h}_{\mathrm{e},k}^{\mathrm{T}}\mathbf{w}_{\mathrm{e},k}\sum_{p=1}^{P}\rho_k^p\sum_{m=0}^{M_x-1}w_{\mathrm{a},k}^{m}h_{\mathrm{a},k}^{m,p}\\ =&\gamma_{\mathrm{e},k}\sum_{p=1}^{P}\rho_k^p\big(\mathbf{h}_{\mathrm{a},k}^{p}\big)^{\mathrm{T}}\mathbf{w}_{\mathrm{a},k}.\end{aligned} \tag{17}$$

Then, substituting $\mathbf{H}_k$ of (9) into (12) yields

$$\begin{aligned}\mathbf{h}_{\mathrm{a},k}^{eq} =&\mathbf{h}_{\mathrm{e},k}^{\mathrm{T}} \otimes \Big(\sum_{p=1}^{P}\rho_k^p\mathbf{h}_{\mathrm{a},k}^{p}\Big)\mathbf{w}_{\mathrm{e},k}\\ =&\mathbf{h}_{\mathrm{e},k}^{\mathrm{T}}\mathbf{w}_{\mathrm{e},k}\sum_{p=1}^{P}\rho_k^p\mathbf{h}_{\mathrm{a},k}^{p} = \gamma_{\mathrm{e},k}\sum_{p=1}^{P}\rho_k^p\mathbf{h}_{\mathrm{a},k}^{p}.\end{aligned} \tag{18}$$

TABLE I
PROCEDURE OF PROPOSED 2D PRECODING SCHEME FOR 3D MIMO

Parameters	The number of users per cell, K, and the dimension of URA, $M_y \times M_x$
Inputs	The 3D channel matrices $\mathbf{H}_k$, $1 \le k \le K$
Step 1	Obtain the approximated elevation steering vector $\overline{\mathbf{h}}_{\mathrm{e},k}$ from the 3D channel matrix (9)
Step 2	2.1: Construct the elevation channel matrix $\overline{\mathbf{H}}_{\mathrm{e}}$ 2.2: Perform the ZF precoding on $\overline{\mathbf{H}}_{\mathrm{e}}$ to obtain the elevation precoding channel matrix $\mathbf{W}_{\mathrm{e}}$
Step 3	Obtain the equivalent azimuth steering vector $\mathbf{h}_{\mathrm{a},k}^{eq}$
Step 4	4.1: Construct the azimuth channel matrix $\overline{\mathbf{H}}_{\mathrm{a}}^{eq}$ 4.2: Perform the ZF precoding on $\overline{\mathbf{H}}_{\mathrm{a}}^{eq}$ to obtain the azimuth precoding channel matrix $\mathbf{W}_{\mathrm{a}}$
Step 5	Calculate the overall precoding matrix $\mathbf{W}_k$ for the k-th user using Kronecker product

Hence $\mathbf{H}_k \oplus \mathbf{W}_k = \left(\mathbf{h}_{\mathrm{a},k}^{eq}\right)^{\mathrm{T}} \mathbf{w}_{\mathrm{a},k} = \gamma_{\mathrm{a},k}$. The computation of $\mathbf{H}_k \oplus \mathbf{W}_{k'}$ for $k' \neq k$ is similar, and we have $\mathbf{H}_k \oplus \mathbf{W}_{k'} = \mathbf{h}_{\mathrm{e},k}^{\mathrm{T}} \mathbf{w}_{\mathrm{e},k'}$. Since $\mathbf{h}_{\mathrm{e},k}^{\mathrm{T}} \mathbf{w}_{\mathrm{e},k'} = 0$ when $k' \neq k$, we have

$$\mathbf{H}_k \oplus \mathbf{W}_{k'} = \begin{cases} \gamma_{\mathrm{a},k}, & k' = k, \\ 0, & k' \neq k. \end{cases} \tag{19}$$

One the other hand, $\mathbf{h}_{\mathrm{vec},k}^{\mathrm{T}} \mathbf{w}_{\mathrm{vec},k'}$ in (2) is given by

$$\mathbf{h}_{\mathrm{vec},k}^{\mathrm{T}} \mathbf{w}_{\mathrm{vec},k'} = \mathbf{H}_k \oplus \mathbf{W}_{k'},\ 1 \le k' \le K. \tag{20}$$

Therefore, the desired signal term in (2) is $\gamma_{\mathrm{a},k} x_k$ and the inter-user interference term becomes zero. Thus the proposed scheme completely eliminates the inter-user interference, despite having only a limited number of antennas in the elevation-domain.

C. Complexity Analysis

Compared to the conventional multiplexing scheme [2], [3], which carries out full TPC based on the channel matrix $\mathbf{H}_k$ or its vectorial form $\mathbf{h}_{\mathrm{vec},k}$ directly, our 2D TPC scheme has a significantly lower complexity. Specifically, it replaces the $M = M_x M_y$-dimensional matrix operations by M_x-dimensional and M_y-dimensional matrix operations based on the Kronecker structure of the channel matrix. It is widely recognized that with a certain number of users K, the computational complexity of the TPC is dominated by the matrix multiplication, which is proportional to the matrix dimension involved. As a direct consequence of exploiting the Kronecker structure of the channel matrix, the $\mathsf{O}(M_x M_y)$ complexity required by the conventional full TPC scheme is reduced to $\mathsf{O}(M_x + M_y)$ in our 2D TPC scheme, which is significant, especially for massive MIMO schemes.

D. Multi-cell Senario

As pointed out previously, our proposed 2D TPC scheme is equally applicable to the multi-cell senario. Let L be the number of cells and K be the number of users per cell, which are served during the same time/frequency resource. Let us denote the downlink channel matrix between the BS of the s-cell and the k-th user in the q-th cell by $\mathbf{H}_{k,q,s} \in \mathbb{C}^{M_y \times M_x}$. The following P-path narrow-band multi-path channel model is considered [14]

$$\mathbf{H}_{k,q,s} = \sum_{p=1}^{P} \mathbf{H}_{k,q,s}^{p}, \tag{21}$$

where $\mathbf{H}_{k,q,s}^{p}$ denotes the p-th path component of the channel matrix. The element at the l-th row and m-th column of $\mathbf{H}_{k,q,s}^{p}$ is given by

$$h_{k,q,s}^{m,l,p} = \rho_{k,q,s}^{p} e^{-\mathrm{j}2\pi \frac{D}{\lambda}\left((m-1)\cos\theta_{k,q,s}^{p}\cos\beta_{k,q,s}^{p} + (l-1)\sin\beta_{k,q,s}^{p}\right)}, \tag{22}$$

where $\theta_{k,q,s}^{p}$ and $\beta_{k,q,s}^{p}$ are the A-AOA and E-AOA of the p-th path, respectively, and the large-scale fading coefficient $\rho_{k,q,s}^{p}$ is given by

$$\rho_{k,q,s}^{p} = \frac{z_{k,q,s}^{p}}{(d_{k,q,s})^{\alpha}}, \tag{23}$$

in which $d_{k,q,s}$ denotes the distance between the BS of the s-cell and the k-th user in the q-th cell, α is the path-loss exponent, and $z_{k,q,s}^{p}$ is the shadow-fading coefficient that follows the log-normal distribution with a variance of σ_z^2.

Under the condition that there are K orthogonal pilots, which are reused in every cell [16], the channel estimation at the BS of the q-th cell is formulated as

$$\widehat{\mathbf{H}}_{k,q,q} = \mathbf{H}_{k,q,q} + \sum_{s \neq q} \mathbf{H}_{k,q,s}, \tag{24}$$

in the absence of AWGN. The BS utilizes the estimate $\widehat{\mathbf{H}}_{k,q,q}$ to obtain the TPC matrix and transmits the downlink data. The ubiquitous pilot-contamination degrades the channel estimate of (24), which imposes inter-cell interference and degrades the overall performance. The following analysis will illuminate, how the 2D TPC deals with this inter-cell interference in order to further improve the overall performance in multi-cell scenarios.

When taking the inter-cell interference into consideration, the elevation channel matrix of (10) is rewritten as

$$\widehat{\overline{\mathbf{H}}}_{\mathrm{e}} = \left[\widehat{\overline{\mathbf{h}}}_{\mathrm{e},1}, \widehat{\overline{\mathbf{h}}}_{\mathrm{e},2} \cdots \widehat{\overline{\mathbf{h}}}_{\mathrm{e},K}\right]^{\mathrm{T}} \in \mathbb{C}^{K \times M_y}, \tag{25}$$

where $\widehat{\overline{\mathbf{h}}}_{\mathrm{e},k} \in \mathbb{C}^{M_y \times 1} = \overline{\mathbf{h}}_{\mathrm{e},k} + \mathbf{h}_{\mathrm{e},k,\mathrm{i}}$ denotes the contaminated elevation channel vector for the k-th user. Thus $\widehat{\overline{\mathbf{H}}}_{\mathrm{e}}$ can be simply decomposed into two parts as follows

$$\widehat{\overline{\mathbf{H}}}_{\mathrm{e}} = \overline{\mathbf{H}}_{\mathrm{e}} + \mathbf{H}_{\mathrm{i}}, \tag{26}$$

where $\mathbf{H}_{\mathrm{i}}$ indicates the inter-cell interference. Then the elevation precoder generated from (11) is rewritten as $\widehat{\mathbf{W}}_{\mathrm{e}} = \widehat{\overline{\mathbf{H}}}_{\mathrm{e}}^{\mathrm{H}} \left(\widehat{\overline{\mathbf{H}}}_{\mathrm{e}} \widehat{\overline{\mathbf{H}}}_{\mathrm{e}}^{\mathrm{H}}\right)^{-1} \widehat{\mathbf{\Gamma}}_{\mathrm{e}} \in \mathbb{C}^{M_y \times K}$. Upon invoking the elevation

precoder, we can obtain the equivalent downlink elevation channel $\mathbf{G}_{\mathrm{e}} = \overline{\mathbf{H}}_{\mathrm{e}}\widehat{\mathbf{W}}_{\mathrm{e}} \in \mathbb{C}^{K\times K}$, which is formulated as follows

$$\begin{aligned}\mathbf{G}_{\mathrm{e}} &= \overline{\mathbf{H}}_{\mathrm{e}}(\overline{\mathbf{H}}_{\mathrm{e}}+\mathbf{H}_{\mathrm{i}})^{\mathrm{H}}\big((\overline{\mathbf{H}}_{\mathrm{e}}+\mathbf{H}_{\mathrm{i}})(\overline{\mathbf{H}}_{\mathrm{e}}+\mathbf{H}_{\mathrm{i}})^{\mathrm{H}}\big)^{-1}\widehat{\mathbf{\Gamma}}_{\mathrm{e}} \\ &= (\overline{\mathbf{H}}_{\mathrm{e}}\overline{\mathbf{H}}_{\mathrm{e}}^{\mathrm{H}}+\overline{\mathbf{H}}_{\mathrm{e}}\mathbf{H}_{\mathrm{i}}^{\mathrm{H}})(\overline{\mathbf{H}}_{\mathrm{e}}\overline{\mathbf{H}}_{\mathrm{e}}^{\mathrm{H}}+\overline{\mathbf{H}}_{\mathrm{e}}\mathbf{H}_{\mathrm{i}}^{\mathrm{H}} \\ &\quad +\mathbf{H}_{\mathrm{i}}\overline{\mathbf{H}}_{\mathrm{e}}^{\mathrm{H}}+\mathbf{H}_{\mathrm{i}}\mathbf{H}_{\mathrm{i}}^{\mathrm{H}})^{-1}\widehat{\mathbf{\Gamma}}_{\mathrm{e}}. \end{aligned} \tag{27}$$

The two parts of $\widehat{\overline{\mathbf{h}}}_{\mathrm{e},k}$ can be formulated in detail as $\overline{\mathbf{h}}_{\mathrm{e},k}(\{\beta_{k,\mathrm{c}}\})$ and $\mathbf{h}_{\mathrm{e},k,\mathrm{i}}(\{\beta_{k,\mathrm{i}}\})$, where $\{\beta_{k,\mathrm{c}}\}$ and $\{\beta_{k,\mathrm{i}}\}$ represent the sets of E-AOAs for the signals impinging from the center cell and from the other cells, respectively. It is critical that the E-AOAs of the rays impinging from the other cells are much smaller at the users than those of the center cell, which implies that the signals will not overlap in the elevation domain. This property can be formulated as

$$\begin{aligned}&\{\beta_{k,\mathrm{c}}\}\cap\{\beta_{k,\mathrm{i}}\}=\varnothing, \\ &\forall\beta_1\in\{\beta_{k,\mathrm{c}}\},\beta_2\in\{\beta_{k,\mathrm{i}}\},\beta_1>\beta_2. \end{aligned} \tag{28}$$

Thus, exploiting the associated asymptotic property, we have

$$\begin{aligned}&\lim_{M_y\to\infty}\overline{\mathbf{h}}_{\mathrm{e},k}^{\mathrm{H}}\mathbf{h}_{\mathrm{e},k,\mathrm{i}}=0, \\ &\lim_{M_y\to\infty}\overline{\mathbf{H}}_{\mathrm{e}}\mathbf{H}_{\mathrm{i}}^{\mathrm{H}}=\mathbf{0}_K, \\ &\lim_{M_y\to\infty}\mathbf{H}_{\mathrm{i}}\overline{\mathbf{H}}_{\mathrm{e}}^{\mathrm{H}}=\mathbf{0}_K. \end{aligned} \tag{29}$$

Then the equivalent channel $\mathbf{G}_{\mathrm{e}}$ can be approximated as

$$\mathbf{G}_{\mathrm{e}}\approx\overline{\mathbf{H}}_{\mathrm{e}}\overline{\mathbf{H}}_{\mathrm{e}}^{\mathrm{H}}(\overline{\mathbf{H}}_{\mathrm{e}}\overline{\mathbf{H}}_{\mathrm{e}}^{\mathrm{H}}+\mathbf{H}_{\mathrm{i}}\mathbf{H}_{\mathrm{i}}^{\mathrm{H}})^{-1}\widehat{\mathbf{\Gamma}}_{\mathrm{e}}. \tag{30}$$

where $\mathbf{H}_{\mathrm{i}}\mathbf{H}_{\mathrm{i}}^{\mathrm{H}}$ is remains non-zero, which indicates that although the inter-cell interference signals cannot be completely eliminated, they can be considerably reduced. Therefore, we can see that $\mathbf{G}_{\mathrm{e}}\approx\widehat{\mathbf{\Gamma}}_{\mathrm{e}}$ and the inter-cell interference is reduced in the elevation domain, which considerably improves the overall performance in our multi-cell scenario in comparison to the conventional TPC algorithms. It is worth pointing out that in combination with the classic down-tilting or beamforming, the inter-cell interference imposed by the pilot reuse can be further reduced [6].

IV. Performance Evaluation

Our numerical results provided in this section reveal the superiority of our proposal. The single-cell scenario is considered in detail, complemented by the portrayal of the inter-cell interference reduction attained in a multi-cell scenario.

A. Single-cell Simulations

The parameters of the simulated single-cell multi-user systems are listed in Table II. The BS is located in the center, whilst the users are randomly dispersed. In the azimuth domain, the users' A-AOA is uniformly distributed in $\left[\theta_c-\delta_\theta/2,\ \theta_c+\delta_\theta/2\right]$, with a mean of θ_c and an angular spread of δ_θ. Similarly, in the elevation domain, the users' E-AOA is uniformly distributed in $\left[\beta_c-\delta_\beta/2,\ \beta_c+\delta_\beta/2\right]$, with a mean of β_c and an angular spread of δ_β. The URA is set to be square, i.e. $M_x=M_y=\sqrt{M}$. We consider downlink data transmission and the proposed 2D TPC scheme is compared both to the existing conventional beamforming scheme [7], [8] and to the conventional full TPC scheme [2], [3].

TABLE II
Parameters of the Simulated Single-Cell Multi-User System

Number of users per cell K	8
Cell radius	250 m
Height of BS	35 m
Path-loss exponent α	3.5
Variance of shadow fading σ_z^2	8 dB
Antenna spacing D	$\lambda/2$
Number of paths P	10
Angle spread of A-AOA δ_θ	180°
Angle spread of E-AOA δ_β	2.5°

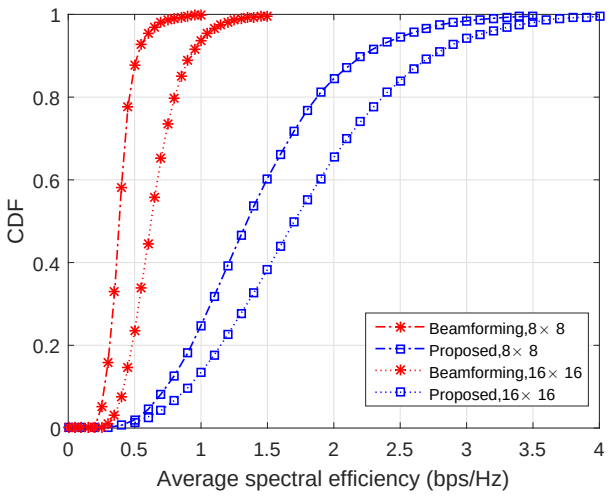

Fig. 2. CDF comparison of downlink average spectral efficiency for proposed scheme and conventional beamforming scheme in *Case 1*. 8×8 and 16×16 URA are adopted.

Case 1. The cumulative distribution function (CDF) of the downlink average spectral efficiency evaluated in the absence of noise is shown in Fig. 2. The full-precoding algorithm is not included here because of its infinite spectral efficiency in the idealized noise-free scenario. Observe in Fig. 2 that the 2D TPC scheme substantially outperforms the conventional beamforming scheme. As the number of antennas per dimension increases, the spectral efficiency of our 2D precoding scheme improves more significantly, since the TPC of the elevation-domain becomes more accurate.

Case 2. In this context the average downlink spectral efficiency achieved at different signal-to-noise ratios SNRs(dB) is presented. Naturally, the full-precoding performs best in the single-cell scenario, since it substantially reduced the inter-user interference, albeit at a high implementation complexity. The other two schemes exploited the Kronecker product structure of the 3D channel matrix, where a somewhat higher inter-user interference persisted.

The derivation of our proposed 2D TPC scheme relies on the approximation of all the elevation-domain channel vectors $\mathbf{h}_{\mathrm{e},k}^{p}$, $1\le p\le P$, by the same approximated elevation-domain channel vector $\mathbf{h}_{\mathrm{e},k}$. The smaller the angular spread

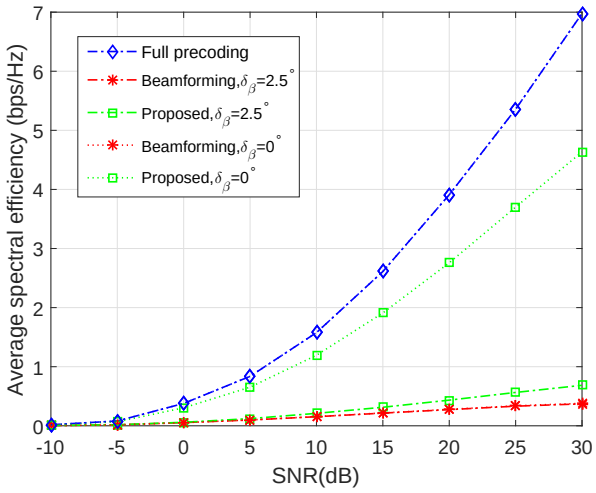

Fig. 3. Comparison of downlink average spectral efficiency for proposed scheme, conventional beamforming scheme and full-precoding in *Case 2*. 8×8 URA is adopted.

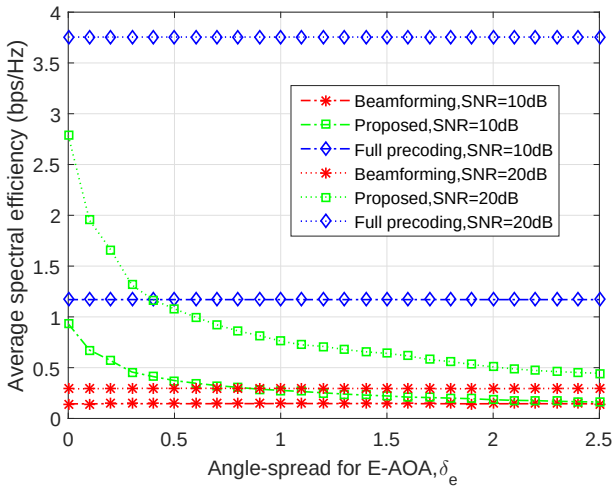

Fig. 5. Comparison of downlink average spectral efficiency for proposed scheme, conventional beamforming scheme and full-precoding in *Case 4* with different angle spreads in elevation domain. 8×8 URA is adopted.

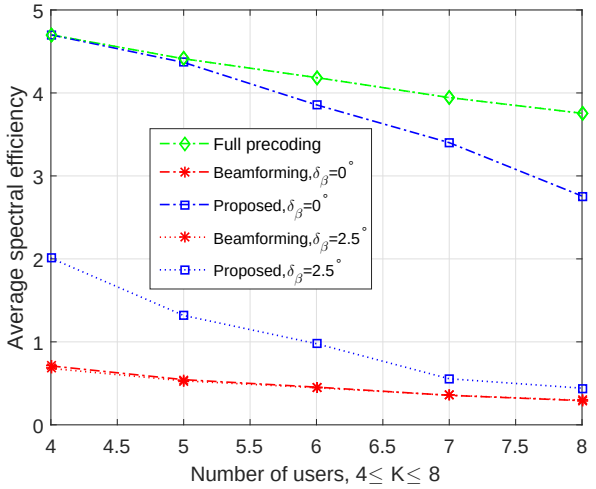

Fig. 4. Comparison of downlink average spectral efficiency for proposed scheme, conventional beamforming scheme and full-precoding in *Case 3* with different number of users K. 8×8 URA is adopted and SNR=20dB.

δ_β of E-AOA, the more accurate this approximation becomes. When we have $\delta_\beta = 0$, the approximation becomes the exact solution. Oserve in Fig. 3 that compared to the case of $\delta_\beta = 2.5°$, our proposal performs much better with $\delta_\beta = 0°$, which approaches the performance of the full-precoding aided scheme.

Case 3. Observe from Fig. 4 that as the number of users increases, the average downlink spectral efficiency reduces for all the schemes due to the higher inter-user interference. Meanwhile, the 2D TPC scheme outperforms the conventional beamforming scheme - regardless of the number of users - owing to its superiority in reducing the inter-user interference.

Case 4. Figure 5 shows our performance comparison of the three algorithms under different angular spreads in the elevation domain. As δ_β increases from $0°$ to $2.5°$, the performance of the 2D TPC rapidly erodes due to the inaccuracy of the channel approximation in the elevation domain, which has been characterized in *case 2* and *case 3*. However, the conventional beamforming scheme is insensitive to δ_β, while the performance of the full-precoding scheme is independent of δ_β. In most scenarios, δ_β is small enough to ensure a high performance for our proposal [15].

B. Multi-cell simulation

The noise-free multi-cell scenario is characterized in this subsection to demonstrate the superiority of our 2D TPC in reducing the inter-cell interference. $L = 7$ cells are considered and the other parameters are the same as in the single-cell scenario. Fig. 6 compares the downlink spectral efficiency achieved by the proposed scheme to those of the conventional beamforming scheme and of the full TPC scheme, where it can be seen that our 2D TPC scheme substantially outperforms the existing beamforming scheme. Furthermore, it can be observed from Fig. 6 that the performance of the existing full TPC scheme is actually worse than that of the existing beamforming scheme in this hostile inter-cell interference environment. Thus, our proposed 2D precoding scheme not only dramatically outperforms the conventional full TPC scheme, but also has a much lower computational complexity.

V. Conclusions

A novel 2D TPC scheme has been proposed for 3D massive MIMO, which performs elevation-domain precoding and azimuth-domain precoding separately by exploiting the Kronecker structure of the 3D MIMO channel. Unlike the conventional beamforming scheme, which fails to completely eliminate the intra-cell or inter-user interference with the aid of a finite number of antennas in the elevation-domain, our proposed scheme fully exploits the degrees of freedom introduced by the elevation-domain antennas for eliminating the inter-user interference. Compared to the existing full TPC scheme, which does not exploit the Kronecker structure of

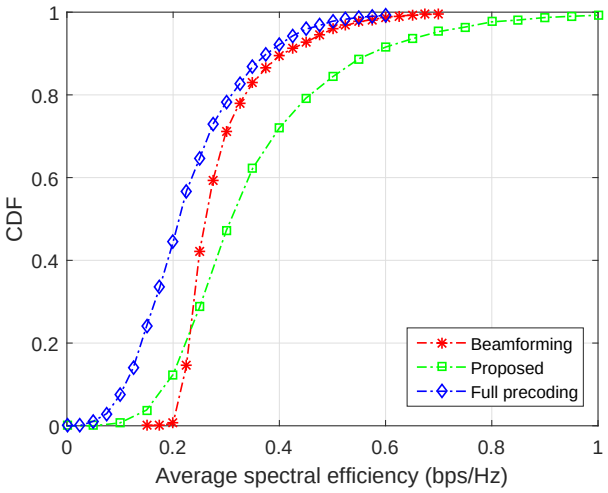

Fig. 6. CDF comparison of downlink average spectral efficiency for proposed scheme, conventional beamforming scheme and full-precoding in multi-cell scenario. 8×8 URA is adopted.

the 3D MIMO channel, our 2D TPC scheme offers a much lower complexity. Our simulation results have verified the superior performance of our proposed scheme over the existing beamforming and full precoding schemes in severe inter-cell interference environments.

REFERENCES

[1] E. G. Larsson, O. Edfors, F. Tufvesson, and T. L. Marzetta, "Massive MIMO for next generation wireless systems," *IEEE Commun. Mag.*, vol. 52, no. 2, pp. 186–195, Feb. 2014.

[2] F. Rusek, D. Persson, B. K. Lau, E. G. Larsson, T. L. Marzetta, O. Edfors, and F. Tufvesson, "Scaling up MIMO: Opportunities and challenges with very large arrays," *IEEE Signal Proc. Mag.*, vol. 30, no. 1, pp. 40–60, Jan. 2013.

[3] T. L. Marzetta, "Noncooperative cellular wireless with unlimited numbers of base station antennas," *IEEE Trans. Wirel. Commun.*, vol. 9, no. 11, pp. 3590–3600, Nov. 2010.

[4] H. Q. Ngo, E. G. Larsson, and T. L. Marzetta, "Energy and spectral efficiency of very large multiuser MIMO systems," *IEEE Trans. Commun.*, vol. 61, no. 4, pp. 1436–1449, Apr. 2013.

[5] Y.-H. Nam, B. L. Ng, K. Sayana, Y. Li, J. Zhang, Y. Kim, and J. Lee, "Full-dimension MIMO (FD-MIMO) for next generation celluar technology," *IEEE Commun. Mag.*, vol. 51, no. 6 pp. 172–179, Jun. 2013.

[6] S. Akoum and J. Acharya, "Full-dimensional MIMO for future cellular networks," in *Proc. 2014 IEEE RWS* (Newport Beach, CA), Jan. 19-23, 2014, pp. 1–3.

[7] Y. Song, S. Nagata, H. Jiang, and L. Chen, "CSI-RS design for 3D MIMO in future LTE-advanced," in *Proc. ICC 2014* (Sydney, NSW), Jun. 10-14, 2014, pp. 5101–5106.

[8] A. Alkhateeby, G. Leusz and R. W. Heath Jr., "Multi-layer precoding for full-dimensional massive MIMO systems," in *proc. of 48th Asilomar Conference on Signals, Systems and Computers, 2014*, Nov. 2-5, 2014, pp. 815–819.

[9] L. You, X. Gao, X.-G. Xia, N. Ma, and Y. Peng, "Massive MIMO transmission with pilot reuse in single cell," in *Proc. ICC 2014* (Sydney, NSW), Jun. 10-14, 2014, pp. 4794–4799.

[10] F. W. Vook, E. Visotsky, T. A. Thomas and B. Mondal, "Product codebook feedback for massive MIMO with cross-polarized 2D antenna arrays," in *Proc. IEEE PIMRC 2014* (Washington DC), Sep. 2-5, 2014, pp. 502–506.

[11] R1-150713, Samsung, "Discussion on FD-MIMO Codebook Enhancments," 3GPP TSG RAN WG1 #80 (Athens, Greece), Feb. 9-13, 201.

[12] R1-150516, NVIDIA, "Performance of Kronecker-based CSI feedback for EBF/FD-MIMO," 3GPP TSG RAN WG1 #80 (Athens, Greece), Feb. 9-13, 2015.

[13] Y.-H. Nam, M. S. Rahman, Y. Li, and J.-Y. Seol, "Full dimension MIMO for LTE-Advanced and 5G," in *Proc. 2015 ITA Workshop* (San Diego, CA), Feb. 1-6, 2015, pp. 1–6.

[14] A. Kammoun, H. Khanfir, Z. Altman, M. Debbah, and M. Kammoun, "Preliminary results on 3D channel modeling: From theory to standardization," *IEEE J. Sel. Areas Commun.*, vol. 32, no. 6, pp. 1219–1229, Jun. 2014.

[15] J. Wang, R. Zhang, W, Duan, S. X. Lu, and L. Cai, "Angular spread measurement and modeling for 3D MIMO in urban macrocellular radio channels," in *Proc. ICC 2014* (Sydney, NSW), Jun. 10-14, 2014, pp. 20–25.

[16] A. Hu, T. Lv, H. Gao, Y. Lu, and E. Liu, "Pilot design for large-scale multi-cell multiuser MIMO systems," in *Proc. ICC 2013* (Budapest, Hungry), Jun.9-13, 2013, pp. 5381–5385.